J. Fluid Mech. (1999), *vol.* 397, *pp.* 259–283. Printed in the United Kingdom

© 1999 Cambridge University Press

The influence of phase on the nonlinear evolution of wavepackets in boundary layers

By MARCELLO A. F. MEDEIROS† AND MICHAEL GASTER‡

Cambridge University Engineering Department, Trumpington Street, Cambridge CB2 1PZ, UK

(Received 23 October 1997 and in revised form 26 May 1999)

The nonlinear evolution of wavepackets in a laminar boundary layer has been observed experimentally. The packets originated from disturbances generated by a loudspeaker coupled to the boundary layer by a small hole in the plate. In a preliminary experiment two types of short-duration acoustic pulses were used, one with a positive excitation and another with a negative excitation. The experiments indicated that the packet that originated from a positive pulse displayed nonlinear behaviour at considerably lower amplitudes than that from a negative pulse. However, the preliminary experiments suggested that at some distance from the source the packets were identical in shape with a relative phase shift of 180°. Using complex-amplitude pulses it was possible to extend the experiments to include packets with other phases. This more comprehensive experiment not only showed a strong influence of the phase on the evolution of the packet, but also demonstrated that this nonlinear behaviour is not determined by the local effects of the excitation process. The observations suggested that the important parameter is the phase of the packet relative to the modulation envelope.

1. Introduction

Transition in boundary layers has been studied for about a century, but there are aspects of the problem that need further investigation. Often the process involves the spatial amplification of waves in the downstream direction. For small amplitudes these waves, known as Tollmien–Schlichting waves, behave linearly, but prior to transition they display nonlinear behaviour. Considerable work has been directed to understanding the nonlinear evolution of these waves. Most of this work has been concentrated on the simpler case of a two-dimensional monochromatic wavetrain. However, the waves that arise in natural transition are in general strongly modulated three-dimensional waves. Despite the practical importance of this topic, this more generic type of waveform has attracted little attention.

An example of the behaviour of modulated Tollmien–Schlichting waves is provided by the study of wavepackets in boundary layers carried out by Gaster & Grant (1975) and Gaster (1975). In that experiment, a point source was used to introduce a pulsed excitation to the boundary layer. The pulse excited a wide band of Fourier modes. The different amplification rates of the various modes created a relatively narrow

† Present Address: Departamento de Engenharia Mecânica, Pontifícia Universidade Católica de Minas Gerais, Av. Dom José Gaspar, 500, Belo Horizonte, 30535-610, MG, Brazil.

‡ Present Address: Department of Mechanical Engineering, Queen Mary & Westfield College, Mile End Road, London, UK.

https://doi.org/10.1017/S0022112099006175 Published online by Cambridge University Press

band of frequencies in the velocity fluctuation spectrum downstream. The various spatial modes combine to form a wavepacket. At very small amplitudes the packet displayed a smooth amplitude distribution and the wave crests were arranged in the form of crescents. Further downstream the hot-wire records showed some distortion in the amplitude distribution and the wave crests became warped across the span. Gaster & Grant observed that the distortions were associated with the growth of oblique waves of frequencies lower than the Tollmien–Schlichting band. As the linear theory did not predict the appearance of these modes (Gaster 1975), they attributed the phenomenon to nonlinear effects.

Perhaps the most surprising result of that work was that the nonlinear manifestation was observed at extremely low amplitudes of the velocity fluctuation within the wavepacket, well below amplitudes at which plane wavetrains begin to display nonlinear behaviour. Later, this result was confirmed with proper comparisons between the evolution of regular wavetrains and wavepackets (Gaster 1978*a*). In these more recent experiments bursts of high-frequency oscillations were observed in the wavepacket at amplitudes for which the regular wavetrain would still be described by linear theory. Similar bursts have also been identified in experimental observations of natural transition (Shaikh 1993). This behaviour suggests that the wavepacket provides a good model of the natural transition process.

A wavepacket similar to that of Gaster & Grant, but of opposite sign, can also be generated if a disturbance of opposite sign, namely a negative-going pulse, is introduced into the boundary layer. Figure 1 displays hot-wire records showing the evolution of the two wavepackets. The evolution is three-dimensional, but here the velocity records were obtained only along the centreline of the flow at a fixed non-dimensional position from the wall. At the first few streamwise stations the velocity records of both wavepackets are identical in shape, but opposite in sign, indicating that the system is a linear one. As the waves travel further downstream the amplitudes increase and the packets become longer. At some station downstream, nonlinear behaviour is evident because the shapes of the packets of opposite excitation signs are no longer identical. In fact, the nonlinear development of these two packets is quite different. The packet created by a positive pulse, here called a 'positive packet', exhibits a much larger growth rate than that of the other one, the 'negative packet'.

The influence of the excitation sign on the evolution of the wavepacket appears to have also been observed by other experimentalists (Gaster 1984; Healey 1995). It is sometimes suggested that this somewhat surprising result can be linked to the local excitation mechanism that will be different for a suction or blowing pulse. A subharmonic resonance mechanism has also been proposed. We have carried out experiments specifically designed to test these conjectures (Medeiros 1996). The current paper is concerned with the local influence of the excitation process. The research indicated that the phenomenon was not determined by the type of the excitation introduced at the source. It appeared that the important factor was the position of the wave ripples relative to the modulation envelope. The experimental investigation of the possibility of resonant interaction is discussed by Medeiros & Gaster (1999), but it can be anticipated that, although subharmonic resonance may be present, it cannot fully explain the observations made here. In the resonance mechanism considered by Healey (1995) higher harmonic signals are predicted, whereas in the current work subharmonics are formed.

The experiments carried out in the present study were of the controlled type, that is, the flow was artificially perturbed to generate the waves that cause transition. The disturbances were generated by a loudspeaker buried in the flat plate over which

https://doi.org/10.1017/S0022112099006175 Published online by Cambridge University Press

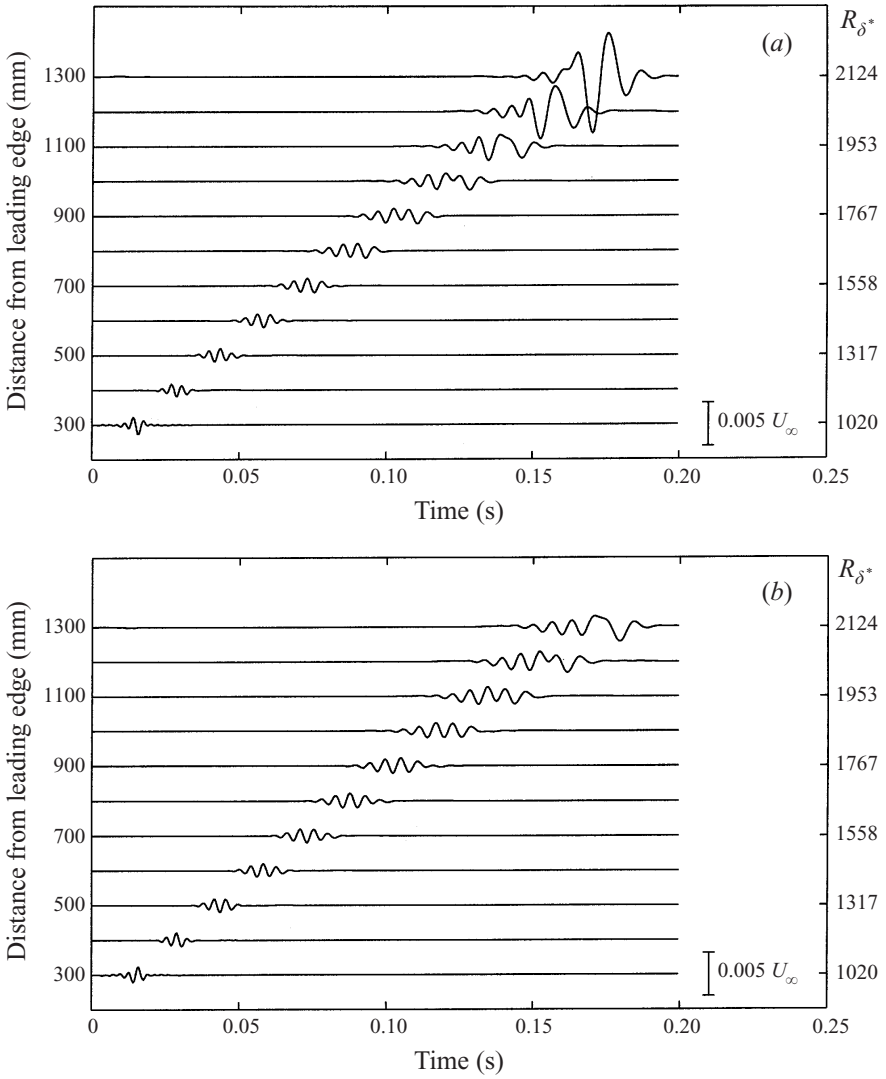


FIGURE 1. Evolution of wavepackets originated from localized pulse excitations shown by hot-wire records on the centreline of the flow at different downstream positions. An indication of the magnitude of the waves is given by the scale shown with the records. (*a*) Positive pulse, (*b*) negative pulse.

the boundary layer developed. These disturbances were communicated to the flow via a small hole. This technique has also been used in many other experiments with wavepackets (Gaster & Grant 1975; Cohen, Breuer & Haritonidis 1991); details of the present experimental set-up and procedures are given in § 2.

With this technique the instability waves are ultimately generated from the movement of the membrane of the speaker. However, the effective nature of the disturbances that perturb the flow has been a subject of controversy, particularly when pulse excitations of opposite signs are used. It has been argued that the movement of the loudspeaker membrane when driven by a positive pulse produces a jet-like disturbance coming out of the hole. On the other hand, when a negative pulse is used, air is sucked into the cavity and the flow disturbance appears as a sink, which

https://doi.org/10.1017/S0022112099006175 Published online by Cambridge University Press

cannot be considered as a negative jet. The difference is that in the case of the jet separation may occur. It has been suggested that the difference in the nature of the disturbance is responsible for the difference in the evolution of the positive and the negative packets. The argument is that in some sense the jet would constitute a more violent disturbance than a sink, introducing more energy to the flow in the form of extra low-frequency noise (J. M. Kendal 1993 and Y. S. Kachanov 1994, personal communications). This would in turn cause the nonlinear interactions to start at an earlier downstream position in agreement with the experimental observations. However, if the excitation mechanism is a linear one, and this must be so for sufficiently small amplitudes, the excitation arises from a normal velocity component on the surface, and there is complete reversibility. We believe that the current experiments operate in this regime.

Another explanation, which also relates to the local effects of the excitation mechanism, has been given for the influence of the sign of the excitation signal. It is known that suction and blowing affect the stability of the boundary layer by distorting the mean velocity profile. Suction causes the profile to be fuller, which is stabilizing, whereas blowing is destabilizing. It has been suggested, therefore, that the disturbances introduced to the flow by the speaker also cause these effects. Following this argument one might conclude that the positive pulse is destabilizing and leads to transition more rapidly than the stabilizing negative pulse, in agreement with experiments (A. Seifert 1995 and V. V. Kozlov 1995, personal communication).

We believe that the disturbances in question are very small indeed and the effects previously described are not likely to be relevant. In fact, experiments by Gaster indicated that at some distance downstream from the source the velocity records of the disturbances originated from the positive and from the negative pulses were identical in shape but opposite in sign. This was considered evidence that whatever the local effects of the excitation mechanism were they had been damped out in the early stages of the evolution of the packet and had not left any scar on the disturbances. On this basis Gaster concluded that the surprisingly large differences in the subsequent nonlinear evolution of the packets were not related to the effects at the source. However, Gaster's measurements were taken outside the boundary layer. It turns out that nonlinear behaviour is more evident when measurements are made within the boundary layer. It is possible that such hot-wire records would have shown differences that could have explained the observations.

An extension to Gaster & Grant's work was carried out (Cohen *et al.* 1991) in which the whole three-dimensional structure of the packet was measured for the three velocity components. The experiments confirmed the conjecture that the evidence of nonlinear activity was much stronger inside the boundary layer than outside. The work states that the oblique waves observed in the nonlinear regime closely satisfied the conditions for resonance of the type proposed by Craik (1971). Unfortunately this comprehensive investigation does not include observations of the wavepacket of opposite sign.

Another series of experiments on localized weak disturbances in boundary layers was carried out by Breuer & Haritonidis (1990). Both experiment and theory showed that, for small enough amplitudes, the disturbances of opposite sign eventually reach a downstream position where the wavepackets are of identical shape but of opposite phase. It was also found that at this Reynolds number the evolution of the packets could be described by linear theory. Unfortunately the experiments did not include the subsequent nonlinear stage of development.

Direct Navier–Stokes computations have also been used to study the nonlinear

https://doi.org/10.1017/S0022112099006175 Published online by Cambridge University Press

evolution of the wavepackets (Konzelmann 1990; Konzelmann & Fasel 1991). The simulations closely reproduced Gaster & Grant's original experiment. In the work of Konzelmann (1990) the growth of the oblique waves was attributed to the secondary instability described by Herbert (1988). More recently, numerical simulations included also the packet generated by a negative pulse (U. Konzelmann 1991, personal communication). Parameters for the simulations were chosen to match new experiments by Gaster. Velocity distributions outside the boundary layer agreed very well with the experiments. Analysis of the results inside the boundary layer indicated that, for the amplitude tested, the disturbances did not reach a stage where they displayed identical shape and opposite signs. Therefore the effect of the source on the nonlinear evolution could not be ruled out, but this contention was unproven.

2. Experimental set-up and procedures

The experimental facility consisted of three main parts, namely the wind tunnel, the controlling computer and a rack of data acquisition modules. The tunnel was well instrumented and allowed the measurement of the fluctuating velocity created by the point excitation. The computer was used to control the experiment and to record the data for future analysis. Communication between the computer and the tunnel was via an IEEE link, which provided control of the Analogue/Digital (A/D) and Digital/Analogue (D/A) converters, voltmeters, filters and stepper motor controllers. With this set-up the computer could therefore be programmed to control the entire experiment, which could be run continuously for many days with very little human interference†.

2.1. *The experimental facility*

All experiments were conducted in the low-turbulence closed circuit wind tunnel at the Cambridge University Engineering Department.‡ The five-bladed low-noise fan was driven by a 25 h.p. motor that was housed separately in an isolated unit designed to reduce the vibration transmitted to the working section. The motor RPM could be specified from the computer and a control loop kept it constant within 0.02%.

The air flow from the fan passed through a gentle diffuser and two sets of turning vanes before going through a 50 mm deep section of paper honeycomb and four fine-mesh screens. It then reached a long settling chamber where the residual turbulence decayed. A rapid 7:1 area ratio contraction accelerated the flow into the working section. The contraction was designed to ensure that the outflow was uniform and that the wall boundary layers stayed attached. The side walls of the $3\times3\times6$ ft working section were slightly divergent (0.4° from the centreline) to compensate for the boundary layer growth on the walls of the tunnel. Even with the model mounted, the flow was very uniform in the working section and the RMS intensity of the free-stream turbulence was typically 0.008% in the frequency range 4 Hz to 4 kHz.

The boundary layer being studied developed over a 1.68 m long flat plate which was mounted vertically on the centre of the working section. The plate was constructed from 12.7 mm thick stress-relieved aluminium. It was fitted with a leading edge with the shape of an integral 9:1 super-elliptic section of degree 3. Care was taken to ensure

† The authors acknowledge the work of Dr T. R. Niew, Dr R. Brandt, Dr F. N. Shaikh, Dr R. Heinrich and Mr S. Bake who, at different levels of participation, installed the instrumentation and control devices and wrote a comprehensive set of basic routines to operate them from the computer.

‡ Now located at Queen Mary & Westfield College, London, UK.

https://doi.org/10.1017/S0022112099006175 Published online by Cambridge University Press

that no noticeable discontinuity existed at the juncture between the leading edge and the plate. A small loudspeaker was buried on the centreline of the plate at 203 mm from the leading edge. The speaker communicated to the flow through a hole of 0.3 mm diameter. Cotton wool was placed between the speaker and the hole in order to prevent extraneous disturbances contaminating the flow. The tunnel was fitted with a three-dimensional hot-wire traverse. It consisted of a two-dimensional traverse system mounted on a side wall-panel which could move vertically for spanwise (z) movement. The panel had a slot along its length which enabled the probe to traverse in the streamwise direction. Probes were moved in the y-direction in and out through the slot. Movement in each direction was provided by lead screws driven by stepper-motors. The whole system was mounted outside the tunnel, with only the probe holder penetrating the working section. In order to diminish the interference to the flow and to reduce the probe vibration, the probe holder was fitted with a fairing in the form of an airfoil.

The traverse system was fully computer operated, but prior to the experiment, the x- and z-positions of the probe were adjusted to line up visually with the position of the disturbance source. The position of the probe relative to the surface of the plate could not be measured directly and had to be inferred from the mean velocity profile which had been shown to be identical to that of the theoretical flat-plate boundary layer solution. It was estimated that this was sufficient to locate the probe within the boundary layer with an accuracy better than 0.01 mm (about 0.02δ).

2.2. *The mean flow characteristics*

The pressure gradient over the plate was measured on an inclined manometer coupled to an array of 0.3 mm diameter static pressure tappings that were distributed along the length of the plate, some distance above the centreline. The overall distribution of pressure over the plate was set by the angle of the plate to the incident flow, but fine adjustment was provided by a flap and a small tab that were mounted at the trailing edge of the plate. With this system an almost zero pressure gradient was obtained and the stagnation point was positioned just on the working side of the plate. A trip wire was attached to the plate just upstream of the first flap in order to ensure that the boundary layer was fully turbulent before passing over the flaps. Another trip wire was attached on the back of the plate at some distance of the leading edge for similar reasons. The plate was sealed to the floor and the ceiling of the working section to prevent flow leakage between the front and the back of the plate.

The values of atmospheric pressure, free-stream velocity and temperature were recorded throughout the experiments and stored. The variation of the free-stream velocity with respect to time was very small. Atmospheric pressure and, in particular, temperature had larger variations throughout the long run time employed. During these experiments the unit Reynolds number varied within $\pm 1\%$.

Velocity profiles were measured by the hot wire at streamwise positions of 300, 500, 700, 900, 1100 and 1300 mm from the leading edge. At each streamwise station the measurements were taken at 21 equally spaced spanwise positions, covering the region ± 200 mm from the centreline of the plate. The results are shown in figure 2 as symbols with the theoretical Blasius profile shown as solid lines. The pressure along the plate was obtained from a number of pressure tappings located off the centerline of the plate. From the pressure measurements and integrating the velocity records to obtain the momentum thickness (θ) the Falkner–Scan parameter ($\Lambda = (\mathrm{d}U/\mathrm{d}x)(\theta^2/\nu)$) was calculated, figure 3.

https://doi.org/10.1017/S0022112099006175 Published online by Cambridge University Press

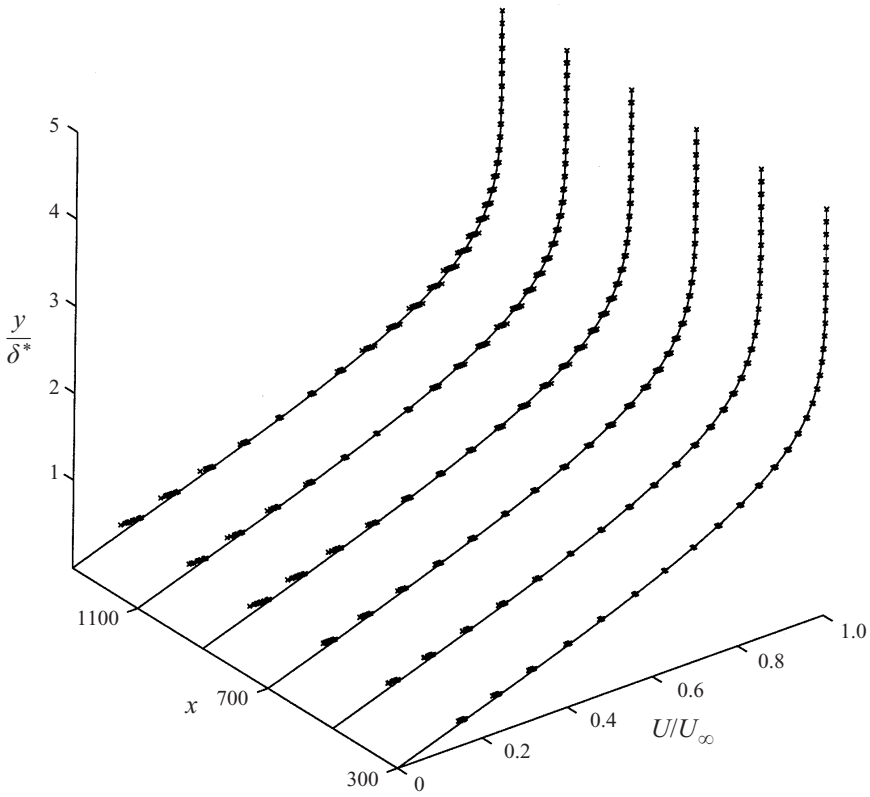


FIGURE 2. The mean flow. The lines represent the theoretical Blasius profile. The symbols represent the experimental profiles.

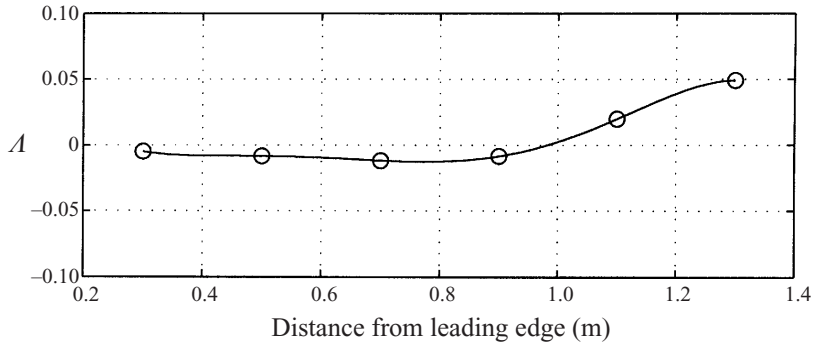


FIGURE 3. The Falkner–Scan parameter distribution.

2.3. *Data acquisition*

Hot-wire anemometry was used to measure the transient flow in the boundary layer on the flat plate. The probe was of the boundary layer type with a 2.5 μm gold plate tungsten wire (Dantec 55P05). This was controlled by a constant-temperature anemometer (Dantec M01) with an overheat ratio of 1.6. The frequency response was adjusted to a maximum of around 30 kHz.

The hot wire was calibrated in the free stream, against the Pitot tube using six

https://doi.org/10.1017/S0022112099006175 Published online by Cambridge University Press

velocity points in the range 5 to 22 m s^{-1}. The semi-empirical King's Law (Perry 1982)

$$E^2 = A + BU^{\alpha} \tag{1}$$

was fitted with minimum square error to the data. In (1), E is the anemometer voltage and U the velocity. Usually α took a value between 0.4 and 0.42. The calibration constants were adjusted by the values of measured temperature and atmospheric pressure.

The output of the hot-wire anemometer was connected to an AC coupled amplifier. The signal was amplified and filtered to remove frequencies above 600 Hz. This was below the Nyquist frequency which, for the sampling rate chosen, was about 700 Hz. The output of the filter was converted to a digital form and stored in the A/D buffer. The time base that controlled the sampling also controlled the D/A converter that was used to drive the power amplifier which drove the speaker to produce the desired controlled disturbances. To improve the signal-to-noise ratio of the hot-wire data 128 ensembles were taken. The standard deviation of the ensembles was also calculated and stored for future use. The 128 wavepackets were triggered at intervals of 0.2 s, which ensured that they behaved like isolated events. The noise below 20 Hz (the fourth Fourier component) was large. Despite the ensemble averaging, this component was not completely removed. In this investigation the interest is focused on relatively high frequencies. Therefore the velocity records were digitally filtered to remove frequencies below 20 Hz.

We were concerned that the analogue signal processing might distort the low-frequency content of the signal. To minimize this effect the impulse response of the circuit containing the AC amplifier and the anti-aliasing filter was measured. This was then used to correct the hot-wire records, but it turned out that the correction was negligible over the frequency range of interest. The signal inevitably contained some noise over the whole record within which the wavepacket was buried. A Fourier analysis of the long record would then be unduly contaminated by the noise. This problem could be overcome by effectively filtering the record with a box-car window that only preserved the wavepacket and set the signal outside the packet domain to zero. The box-car window had smooth ends and different widths according to the size of the packet.

To reconstruct the entire velocity record the mean hot-wire voltage of the undisturbed flow was also necessary and was obtained with a 16 bit A/D converter. In the procedure, the part of the unsteady signal that was windowed out of the wavepacket was used as representative of the undisturbed mean flow.

3. Experiments

3.1. *Preliminary experiments*

In previous experimental studies of the evolution of wavepackets, different types of functions were used to control the pulse that drove the loudspeaker. In Gaster & Grant's original experiment the pulse was rectangular with controlled width. Cohen *et al.* (1991) used a single period of a sinusoid with the frequency of the most unstable mode. In the simulations by Konzelmann (1990) a Gaussian function was used. It appears that in all cases the excitation modelled a narrow pulse excitation very well. In the present series of experiments a different approach was taken. Here, the time series used to drive the speaker were constructed from a combination of a number of

https://doi.org/10.1017/S0022112099006175 Published online by Cambridge University Press

discrete Fourier modes that can be expressed by

$$q(t) = \mathrm{Re}\left\{ a \sum_{m=1}^{m=n} \mathrm{e}^{2\pi \mathrm{i} m f_o t} \right\}. \tag{2}$$

In (2) t varies in the range

$$-\frac{1}{2f_o} < t \leqslant \frac{1}{2f_o}$$

and Re indicates that only the real part of the summation is to be considered. In the limit as the frequency discretization f_o tends to zero and n tends to infinity, $q(t)$ approaches a delta function; f_o was chosen to be 5 Hz. The sampling rate selected for the data acquisition allowed the resolution of 128 Fourier modes, and, because of this, n in equation (2) was taken as 128. The tunnel speed was set to 17.4 m s^{-1}. Measurements were taken on the centreline of the flow at two different distances from the wall, namely $y = 0.6\delta^*$ and $3.5\delta^*$ (where δ^* is the displacement thickness), which roughly correspond, over the parameter range of the data, to the inner and the outer maxima of the streamwise perturbation velocity profile in the linear regime.

The current experiments showed that it was possible to perturb the flow with excitations composed of discrete frequencies and obtain wavepackets identical to those obtained from other excitations that model a pulse. For the excitation amplitudes studied, at a distance of 200 mm from the source the wavepackets of opposite sign were identical in shape when measured outside the boundary layer. Inside the boundary layer, however, the near-field influence extended much further downstream. It was also observed that the linear and nonlinear activities were concentrated at frequencies well below 300 Hz. The peak amplitude of the pulse excitation was then reduced by excluding the modes with frequency above 400 Hz in the time series, that is, using $n = 80$ in equation (2). Modes above this decay very rapidly from the source and their exclusion only reduced the extent of the local effects of the excitation process.

Results of this experiment are displayed on figure 4 for the measurements taken inside the boundary layer. For each excitation amplitude and downstream position two hot-wire records are shown. The solid lines are the signals originating from the positive pulse whereas the dotted lines represent the signals from the negative excitation, which are inverted to facilitate comparison. In the picture an indication of the magnitude of the perturbation velocities involved is given by a scale shown with the records at station $x = 300$ mm. The excitation amplitude, represented by the vertical axis, is proportional to the peak voltage of the signal driving the loudspeaker, and is not necessarily proportional to the amplitude of the disturbance introduced to the flow. The figure shows that for the first streamwise stations the signals are indistinguishable from each other, indicating a linear regime. At $x = 900$ mm, for medium and large excitation amplitudes, large differences between the signals of opposite sign are observed, which indicate nonlinear behaviour. Some differences can also be identified at stations $x = 500$ and 700 mm. To illustrate the results more clearly, the signals marked with an asterisk are shown to a larger scale in figure 5. It is interesting to note that the magnitude of the streamwise perturbation velocity for which the first signs of nonlinearity are detected is roughly 0.2% of the free-stream velocity. This is substantially below the 1% amplitude level for which nonlinearity takes place in experiments with regular plane wavetrains.

To assess the extent to which the records of opposite signs can be considered identical, the linear correlation between these records was calculated for each streamwise

https://doi.org/10.1017/S0022112099006175 Published online by Cambridge University Press

https://doi.org/10.1017/S0022112099006175 Published online by Cambridge University Press

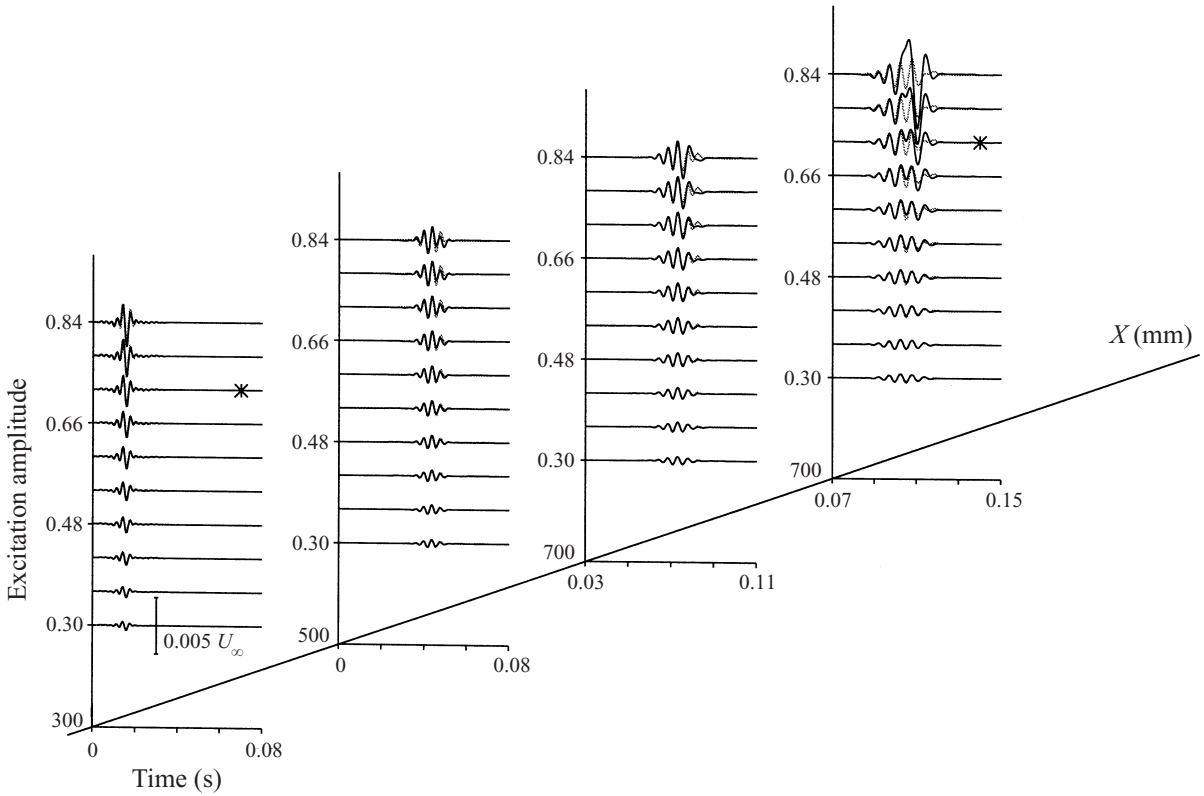


FIGURE 4. Comparison of the evolution of wavepackets originated from positive and negative pulse excitations for different excitation amplitudes. Solid lines correspond to positive pulse, dotted lines, negative pulses. The negative pulse records are inverted to facilitate comparison.

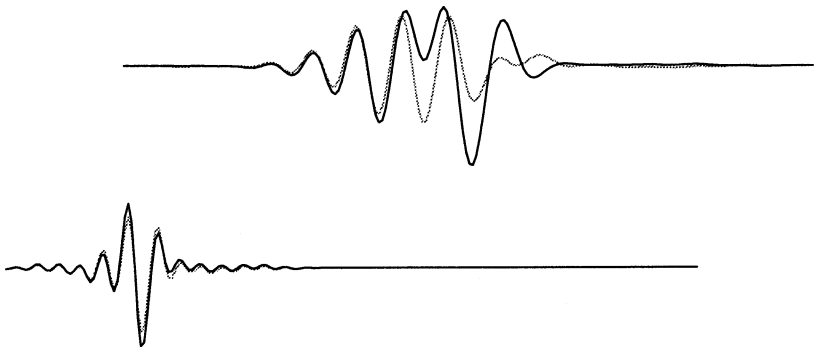


FIGURE 5. Expanded view of the hot-wire records marked with an asterisk on figure 4.

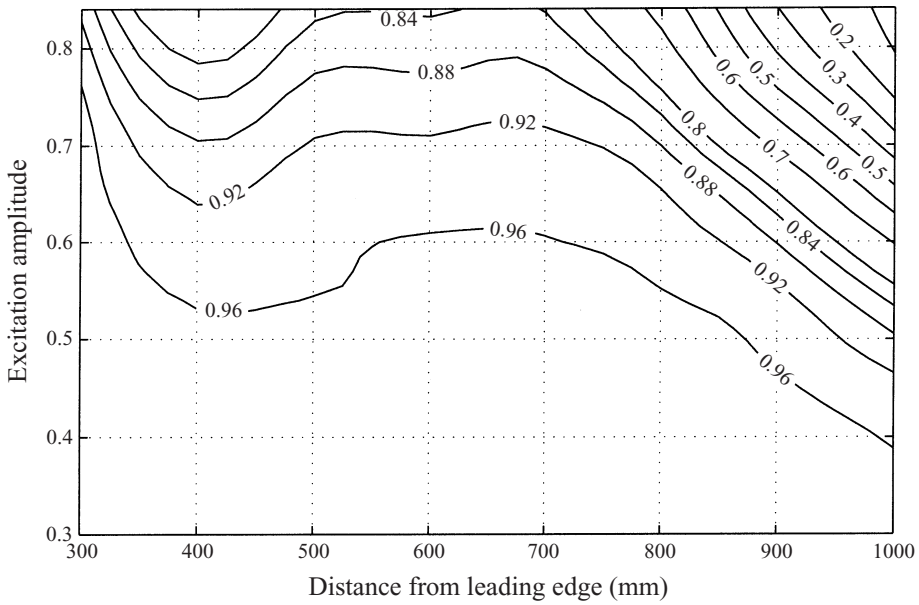


FIGURE 6. Linear correlation between hot-wire records of disturbances generated from positive and negative pulse excitations.

station and excitation amplitude, figure 6. The figure also includes measurements at stations $x = 400$, 600 800 and 1000 mm. The correlation levels are very high considering that they are constructed from experimental velocity records of weak velocity fluctuations. At $x = 400$ and 500 mm a distinct drop in the correlation levels occurs. At $x = 600$ to 700 mm the evolution of the packets can confidently be considered linear for excitation amplitudes 0.6 and below. The sharp drop in the correlation levels around the top-right corner of the figure corresponds to the nonlinear effects with which this research is concerned. In this region, the positive and negative signals are quite different as shown in figure 4. As expected, the lower the amplitude the further downstream the disturbances remain linear. For large excitation amplitudes the local effects of the excitation mechanism are expected to extend further downstream and the nonlinear effects to start further upstream. This may offer an explanation of the fact that the correlation levels for high-amplitude signals did not reach the levels observed for small and medium amplitudes. The nonlinear evolution of the

https://doi.org/10.1017/S0022112099006175 Published online by Cambridge University Press

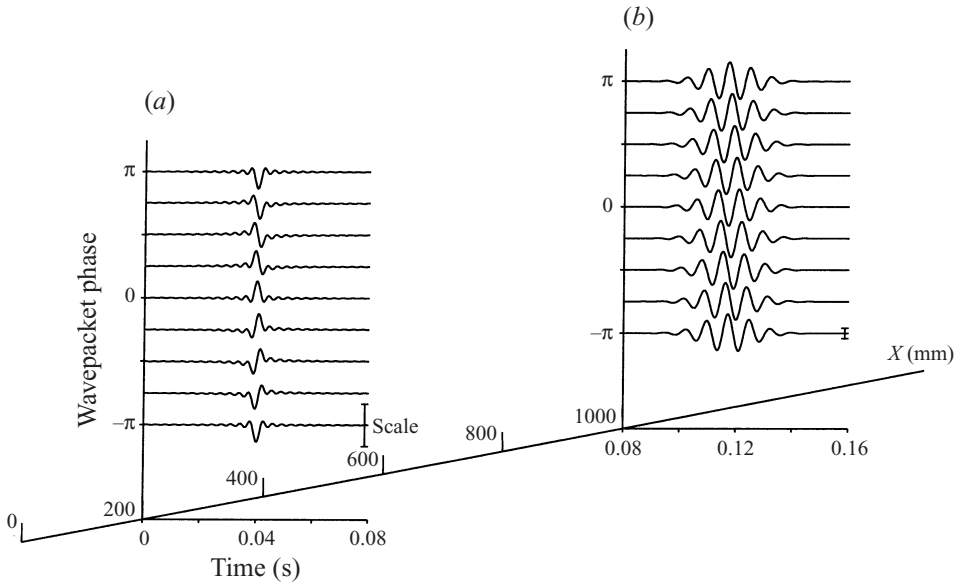


FIGURE 7. (*a*) Excitation time series for different phases and (*b*) theoretical predictions of the two-dimensional linear response of the boundary layer.

packets generated from excitation amplitude 0.6 are shown in figure 1. Considering the correlation levels that the signals attain at streamwise positions 600 and 700 mm it appeared that the differences in the nonlinear regime of the waves were not to be attributed to local effects of the excitation process.

3.2. *The complex wavepacket*

It seemed from this preliminary experiment that the differences observed in the nonlinear evolution of the packets were caused solely by the sign difference of the excitation. The sign of the excitation manifests itself in the distribution of the valleys and peaks (or ripples) of the waveform with respect to an identical amplitude modulation (or envelope). Using the positive and negative pulse excitations, two such ripple dispositions are created, but other distributions are also possible. One way to obtain other ripple dispositions is to allow a in equation (2) to be complex. In this case the excitation time series are given by

$$q(t) = \mathrm{Re}\left\{\hat{a}\mathrm{e}^{\mathrm{i}\phi}\sum_{m=1}^{m=n}\mathrm{e}^{2\pi\mathrm{i}mf_o t}\right\}, \tag{3}$$

where $\hat{a}$ is real. For $\phi = 0$ and $\phi = \pi$ the positive and negative pulse excitations are reproduced. For other values of ϕ packets with other ripple dispositions are excited. Excitation time series for different values of ϕ are shown in figure 7, demonstrating how they change from a negative pulse (π) to a positive pulse (0). The process is obviously periodic in ϕ and the time series for $\phi = \pi$ is repeated at $\phi = -\pi$ to emphasize this cyclic character.

Two-dimensional linear calculations were performed to compute the response of the boundary layer at $x = 1000$ mm to the excitations of the form (3) introduced at a distance of 200 mm from the leading edge. The results are also shown in figure 7. In the calculations of the linear response the series dispersion model developed by

https://doi.org/10.1017/S0022112099006175 Published online by Cambridge University Press

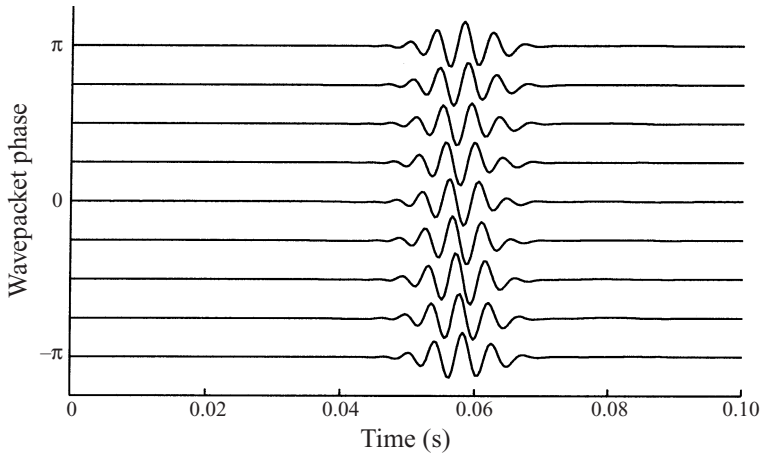


FIGURE 8. Hot-wire records of wavepackets of different phases taken on the centreline of the flow at $y = 0.6\delta^*$. Excitation amplitude 0.6 and downstream station $x = 600$ mm.

Gaster (1978*b*) was used in a double summation over the streamwise wavenumber and the Reynolds number to represent the packet. In this model the receptivity of all modes is assumed to be the same. The results illustrate the variation of the ripple disposition with the wavepacket phase ϕ. The disturbance amplification can also be evaluated from the plots. As the amplification rates were very large the plots had to be re-scaled as indicated.

An experiment similar to that discussed in the previous section was then set up to test this approach. The object was to demonstrate that the wave-maker could produce packets of the required characteristics in the linear regime. Figure 8 displays hot-wire records of the disturbances generated by the different time series. The results correspond to excitation level 0.6 and streamwise position 600 mm, which, from figure 6, are within the linear regime. The variation of the ripple disposition with ϕ is very similar to that shown in figure 7 showing that the technique worked very well.

More definitive information about the characteristics of the different packets is shown in the Fourier domain. The signals are largely dominated by the Tollmien–Schlichting band of frequencies, and the energy in this band is very similar for all packet phases, figure 9. It is possible that the scatter around frequency index 20 is deterministic and due to the phase shifting causing different nonlinear behaviour. This may cast some doubt on whether the disturbances have reached a linear regime even though the correlation levels were very high. In such a case the local influence of the excitation process could not be ruled out. However, as will become clearer at the end of the paper, the nonlinear behaviour is not caused by local effects of the excitation process.

The phase of a number of Fourier components in the packets is shown in figure 10 for packets of different phase. The Fourier components correspond to the even frequency index from 40 to 58. The linear theory predicts a linear variation of the phase of the Fourier components with respect to the phase of the packet (ϕ in equation (3)). This was confirmed by the experiment, figure 10.

3.3. *Nonlinear complex wavepackets*

Having established the characteristics of the packets in the linear regime, the experiment was extended to the nonlinear stages of the process. The first important

https://doi.org/10.1017/S0022112099006175 Published online by Cambridge University Press

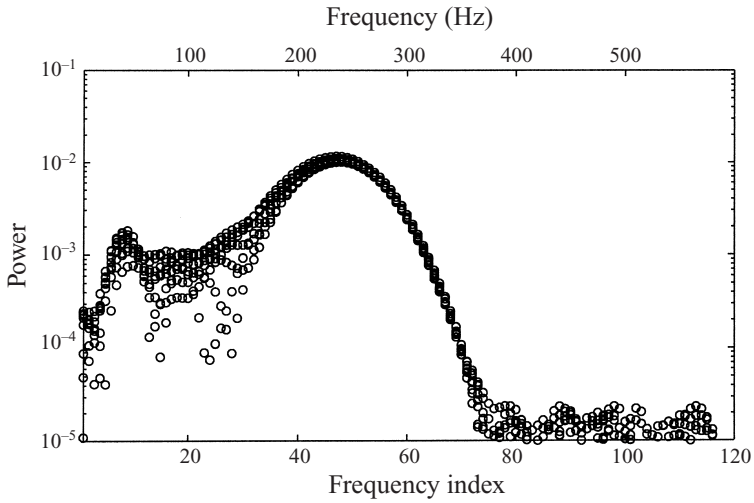


FIGURE 9. Comparison of the spectral content of wavepacket signals of different phases taken on the centreline of the flow at $y = 0.6\delta^*$. Excitation amplitude 0.6 and downstream station $x = 600$ mm.

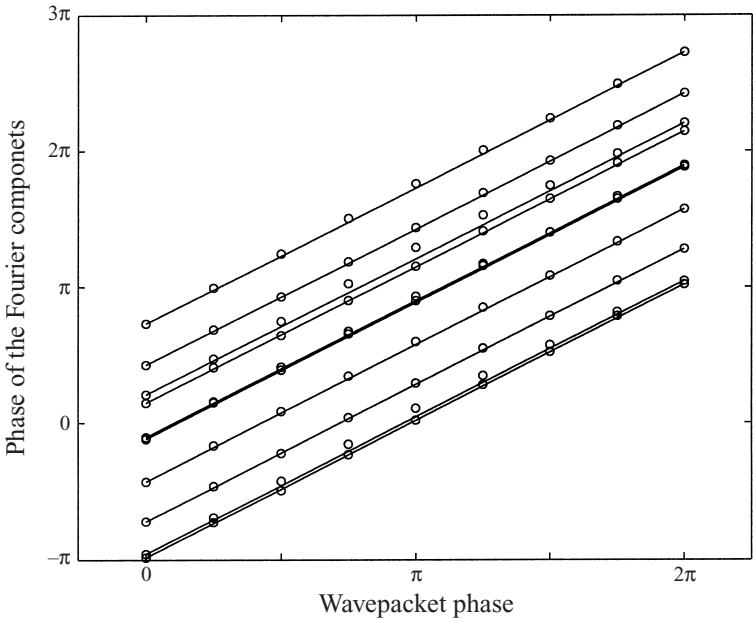


FIGURE 10. Variation of the phase of the dominant Fourier components with respect to the phase of the packets. The solid lines correspond to the theoretical predictions.

result was that the nonlinear interaction is first detected inside the boundary layer. Therefore, the discussion concentrates on the results obtained inside the boundary layer. Measurements of velocity fluctuations are displayed in plots similar to that of figure 8 for a number of downstream stations, building up a three-dimensional picture, figure 11. Because of the large amplification rates, the plots for the last two streamwise stations had to be re-scaled as indicated in the figure. The nonlinear mechanism manifests itself through a distortion of the record that is linked to the loss

https://doi.org/10.1017/S0022112099006175 Published online by Cambridge University Press

https://doi.org/10.1017/S0022112099006175 Published online by Cambridge University Press

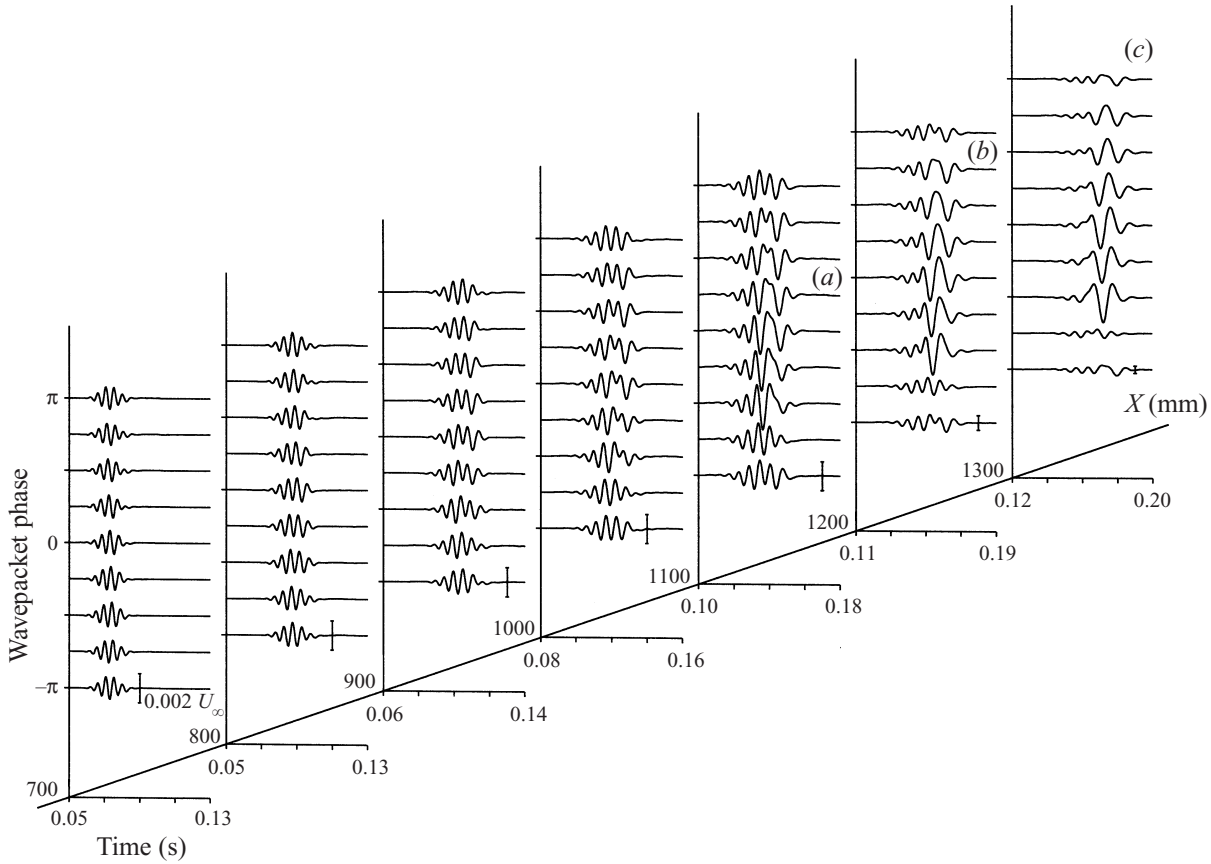


FIGURE 11. Nonlinear evolution of wavepackets of different phases shown by hot-wire records taken on the centreline of the flow at $y = 0.6\delta^*$. Excitation amplitude 0.6.

of one of the fundamental periods at the trailing edge of the packet. At each station the degree of distortion varies substantially with the excitation phase. It appeared that the nonlinear interaction was stronger for phases around 0 whereas the phase $-\frac{3}{4}\pi$, for example, seemed to maintain a linear behaviour for longer downstream distances. The similarities between the wavepacket at $x = 1100$ mm, $\phi = \frac{1}{4}\pi$, labelled (a) in the figure, at $x = 1200$ mm, $\phi = \frac{3}{4}\pi$, labelled (b) and at $x = 1300$ mm, $\phi = \pi$, labelled (c), for example, suggest that the different packets go through similar stages of nonlinear development, but at different downstream positions, depending on the phase of the ripples. The variation of the amplitude of the nonlinear signals with the phase of the packet, most clearly observed at the last streamwise station, indicates that the nonlinear interaction increases the local amplification rates of the disturbances. At stations $x = 1200$ and 1300 mm, for example, the strongly nonlinear packets appear to lose another fundamental period, but this time at the leading edge. Attention is drawn to the fact that the nonlinear behaviour observed occurred at extremely low amplitudes of the streamwise disturbance velocities, of approximately 0.2% peak to peak of U_∞. In regular plane wavetrains nonlinear behaviour usually starts at around a level of 1%.

The records in figure 11 can be expressed as a Fourier series of 128 terms

$$u(j) = \mathrm{Re}\left\{\sum_{m=0}^{m=128} C_m \mathrm{e}^{2\pi \mathrm{i} m j/128}\right\}, \tag{4}$$

where $u(j)$ is the record which is known at $j = 0, 1, 2, \ldots 255$ locations. The coefficients C_m are obtained by the discrete inversion transform. The imaginary part of equation (4) represents a similar wavepacket, but with a phase shift of 90°. The amplitude function, or envelope, of the packet can be obtained by a combination of the real and imaginary parts $[u_r^2(j) + u_i^2(j)]^{1/2}$. The envelopes provide a clearer view of the distortions in the packet, figure 12.

At first the nonlinear signature consisted of a 'dimple' present in the packets with phase around 0. As the nonlinearity develops the dimple evolves into a deep valley. Not only the depth but also the position (time) of the valley varies with the packet phase, as is indicated by the dotted lines for station 1000 mm. It appears that the distortion is connected with a particular ripple of the packet. Initially only one valley was observed at the trailing edge, but further downstream a similar effect also occurred at the leading edge.

More information concerning the nonlinear evolution of the packets can be gained from the power spectra of the signals, figure 13. Again the records at the last two stations had to be re-scaled to fit the picture. At the first station the energy is entirely concentrated in the Tollmien–Schlichting band, indicating a linear regime. As the packets travel downstream the nonlinearity appears as a band of frequencies lower than that of the Tollmien–Schlichting waves. No signal energy appeared in the higher harmonics of the fundamental frequencies. For the strongly nonlinear wavepackets the low-frequency band was the dominant part of the signal, but some energy was still present in the Tollmien–Schlichting band, which was little affected by the nonlinear behaviour. In the Fourier domain the variation of the degree of nonlinearity with respect to the phase of the packet can be better assessed. For the conditions in which this experiment was carried out it appeared that the nonlinearity was most intense for phases around 0 and least intense for the phase $-\frac{3}{4}\pi$.

Another series of experiments was carried out to investigate how the nonlinear interaction varies with the magnitude of the excitation. The hot wire was placed

https://doi.org/10.1017/S0022112099006175 Published online by Cambridge University Press

https://doi.org/10.1017/S0022112099006175 Published online by Cambridge University Press

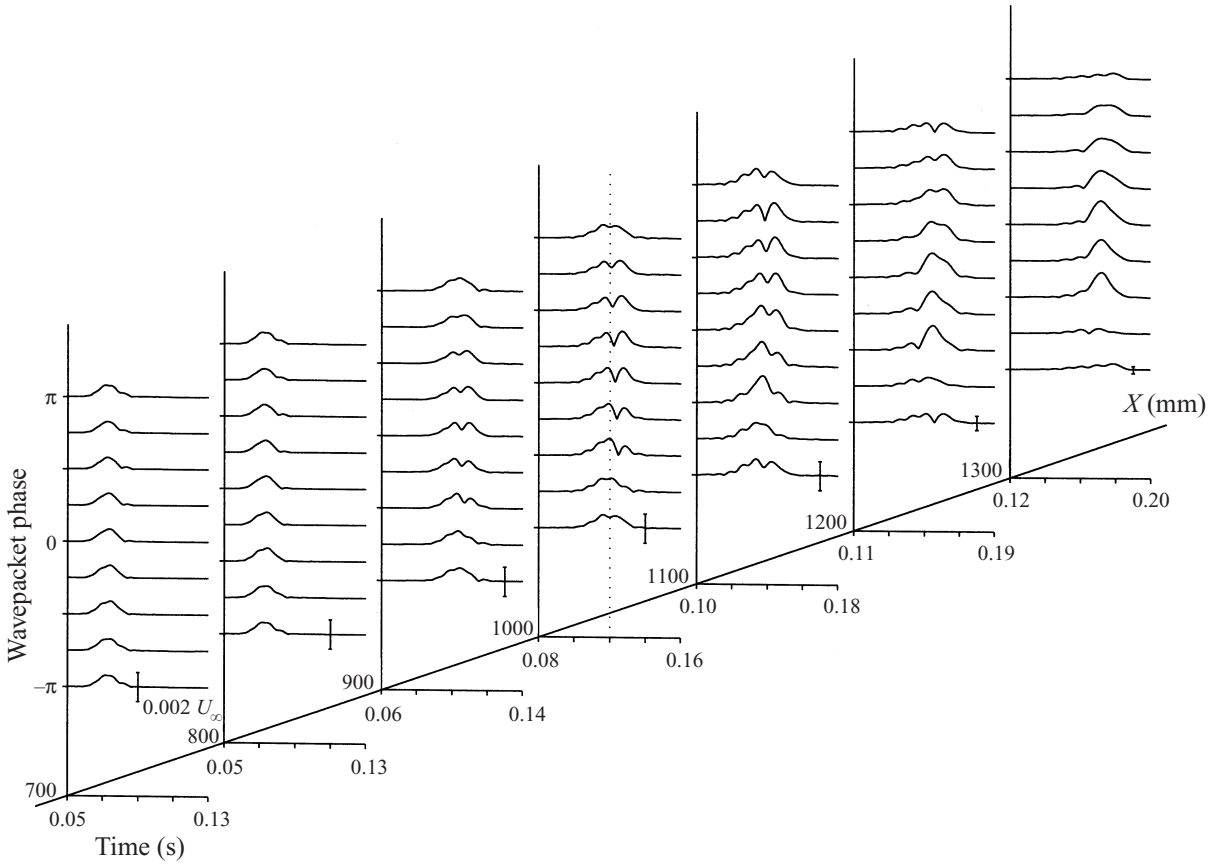


FIGURE 12. Nonlinear evolution of wavepackets of different phases shown by the envelopes of the hot-wire records taken on the centreline of the flow at $y = 0.6\delta^*$. Excitation amplitude 0.6.

https://doi.org/10.1017/S0022112099006175 Published online by Cambridge University Press

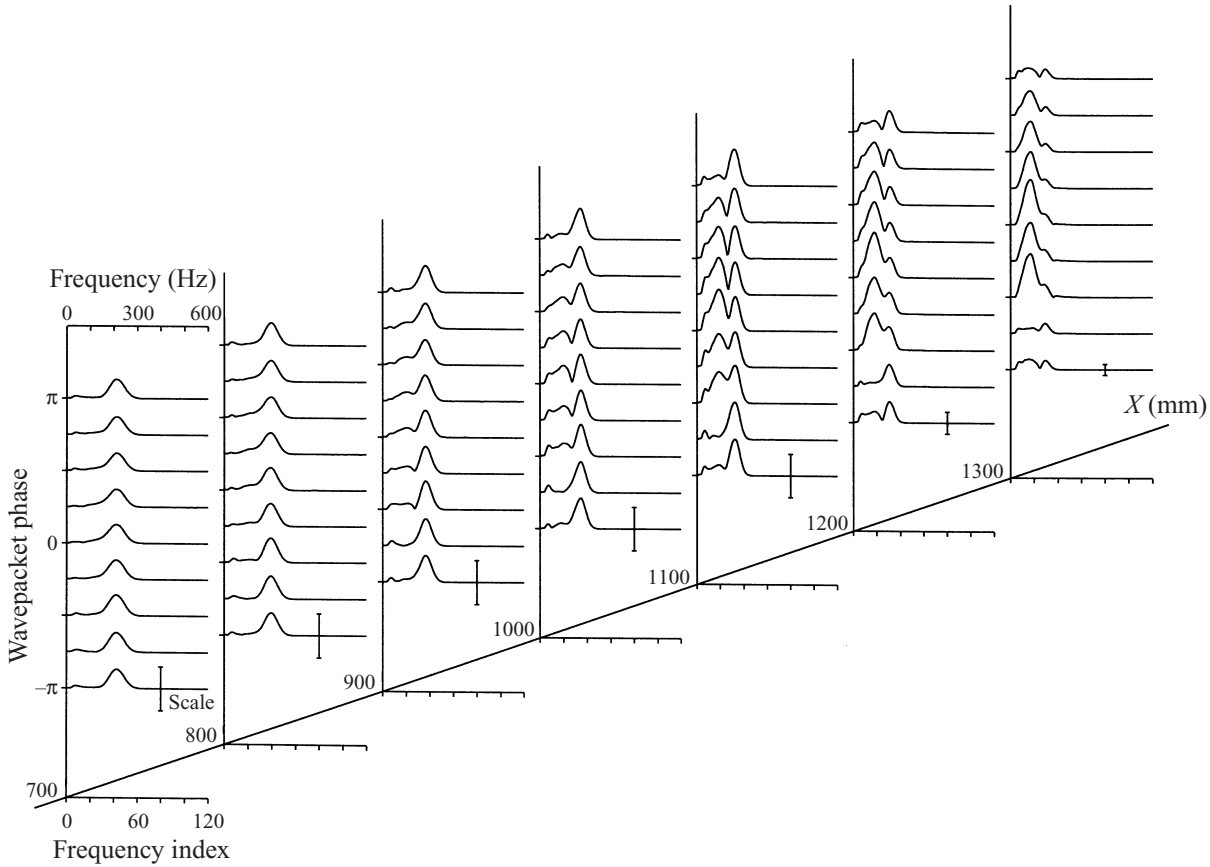


FIGURE 13. Nonlinear evolution of wavepackets of different phases shown by the spectral content of hot-wire records taken on the centreline of the flow at $y = 0.6\delta^*$. Excitation amplitude 0.6.

https://doi.org/10.1017/S0022112099006175 Published online by Cambridge University Press

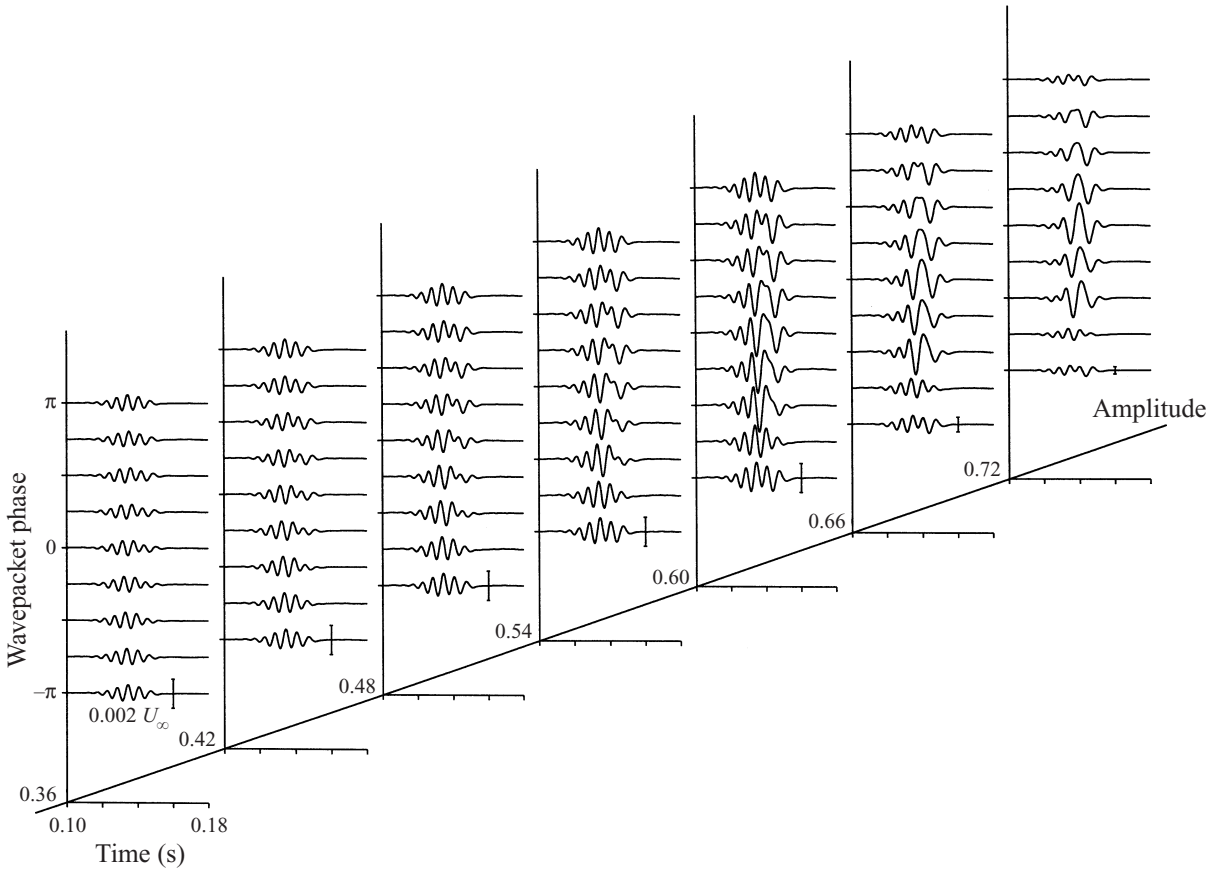


FIGURE 14. Comparison of the nonlinear response of wavepackets of different phases for different excitation levels at downstream station $x = 1100$ mm. The hot-wire records were taken on the centreline of the flow at $y = 0.6\delta^*$.

https://doi.org/10.1017/S0022112099006175 Published online by Cambridge University Press

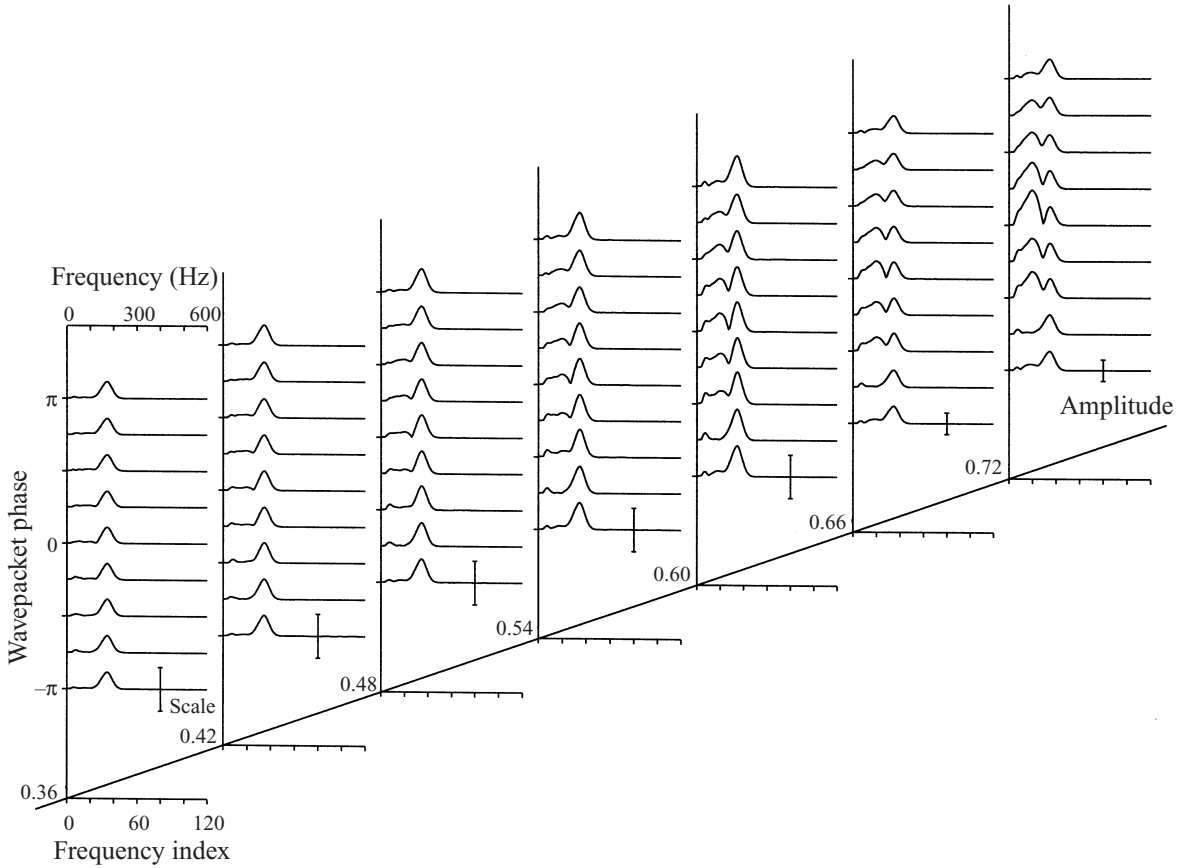


FIGURE 15. Comparison of the spectral content of the signals shown in figure 14.

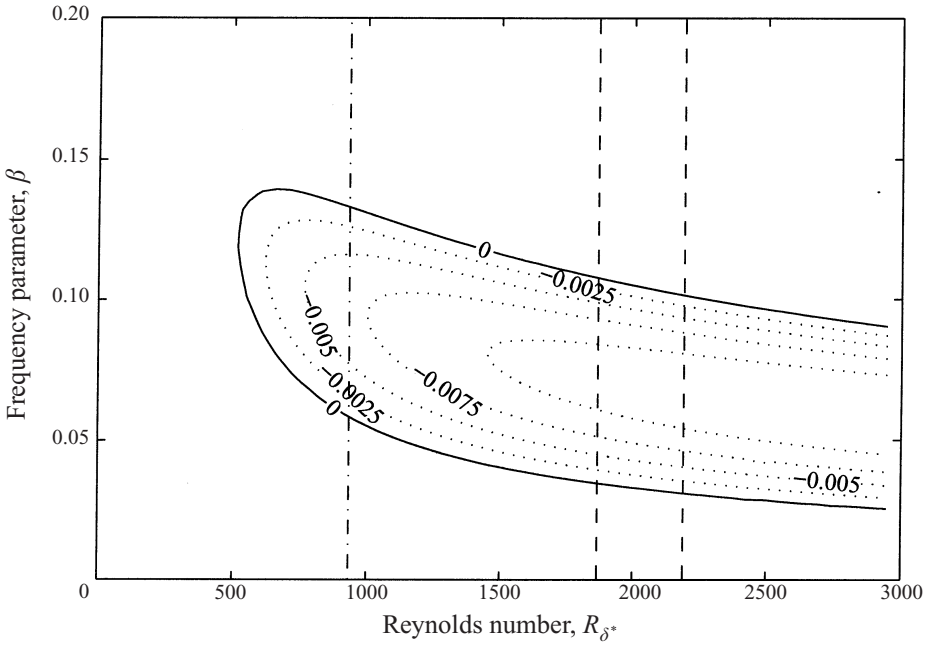


FIGURE 16. Instability diagram for the boundary layer. The dashed-dotted line indicates the value of Reynolds number at the excitation point. The dashed lines indicate the region where the measurements in the nonlinear regime were taken.

at a position downstream from the source and the speaker was driven by the time series defined by equation (3) for different values of $\hat{a}$. The signals obtained are displayed in figure 14 and closely resemble those shown in figure 11. The power spectra of the records, figure 15, resemble those displayed in figure 13. Similar results were obtained for other streamwise stations. It appeared that the variation of the excitation amplitude did not affect the nature of the nonlinear mechanisms, but only shifted the entire process upstream as the amplitudes were increased. This was also noted by Cohen *et al.* (1991).

From figure 15 it appeared that the energy in the low-frequency band that is formed in the nonlinear regime could provide some comparative measure of the intensity of the nonlinear interaction. Assigning to each wavepacket of figure 15 a number associated with the low-frequency band energy could summarize the results in a kind of nonlinear intensity function dependent on amplitude and phase of the excitation, that is, the complex excitation amplitude. It was also found that similar behaviour occurred at lower (12 m s^{-1}) and higher (22 m s^{-1}) free-stream velocities. In the following we report the results obtained with free-stream velocity of 22 m s^{-1} because, as they covered a wider range of Reynolds number, they provide a clearer picture of the aspects to be discussed hereafter.

For this experiment, measurements were taken for 16 different excitation phases and seven excitation magnitudes from 0.16 to 0.52. For all the excitation amplitudes used the packets were found to behave linearly at $x = 700$ mm, as indicated by the linear correlation between the positive and the negative wavepackets which reached levels of 0.98. From station $x = 800$ mm to station $x = 1100$ mm, some nonlinear behaviour was observed. The range of Reynolds number corresponding to the measurements in the nonlinear regime is given by the dashed lines plotted on the

https://doi.org/10.1017/S0022112099006175 Published online by Cambridge University Press

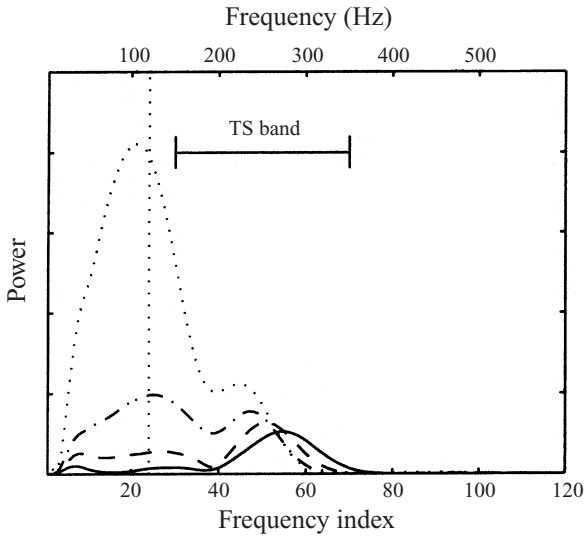


FIGURE 17. Evolution of the wavepacket generated from a positive pulse excitation shown by power spectra of hot-wire records at different downstream locations. Solid line, $x = 800$ mm; dashed line, $x = 900$ mm; dashed-dotted line, $x = 1000$ mm; dotted line, $x = 1100$ mm. The vertical dotted line indicates the Fourier component chosen to construct the diagrams of figure 18.

boundary layer instability diagram shown in figure 16. Also, the value of Reynolds number at which the excitations were introduced to the flow is indicated by the dot-dashed line. Figure 17 shows the evolution in the Fourier domain of a positive wavepacket. It appeared that the magnitude of a Fourier component of frequency close to that of the dominant component of the low-frequency band could give enough of an indication of the energy content in that band. Based on the evolution of the positive wavepacket the 25th Fourier component was chosen for indicating the energy content in the low-frequency band of the different packets. In fact, similar behaviour was found for other components around the 25th. Therefore, the magnitude of the 25th Fourier component was taken as a comparative measure of intensity of the nonlinear interaction of the different packets. The comparative measure of intensity of the nonlinear interaction was obtained for all the excitation phases and amplitudes and the results were then mapped onto the complex-amplitude excitation plane. The results are shown for a number of downstream stations by contour polar plots, with the radius representing the amplitude ($\hat{a}$) and the angle representing the phase (ϕ) of the excitation, figure 18.

A number of important characteristics of the nonlinear phenomenon being studied are represented in figure 18. For instance, the fact that the outer contours are higher than the inner ones indicates that the magnitude of the nonlinear interaction increases with the amplitude of the excitation. The dependence of the nonlinear phenomenon on the phase of the excitation manifests itself in the asymmetry of the contours. The contour level 0.025 at $x = 800$ mm, for example, indicates that the nonlinear interaction is weakest for the phase $-\frac{3}{4}\pi$, which requires almost twice the amplitude to reach the same nonlinear intensity level of the packet of phase shifted by π. The figures convey the idea that at a given downstream station the contour levels are rotated which respect to one another. This is remarkably clear at $x = 1000$ mm. The interpretation of this is as follows. It has been shown above that the variation of the magnitude of the excitation shifts the nonlinear process in the streamwise direction. Now, what

https://doi.org/10.1017/S0022112099006175 Published online by Cambridge University Press

https://doi.org/10.1017/S0022112099006175 Published online by Cambridge University Press

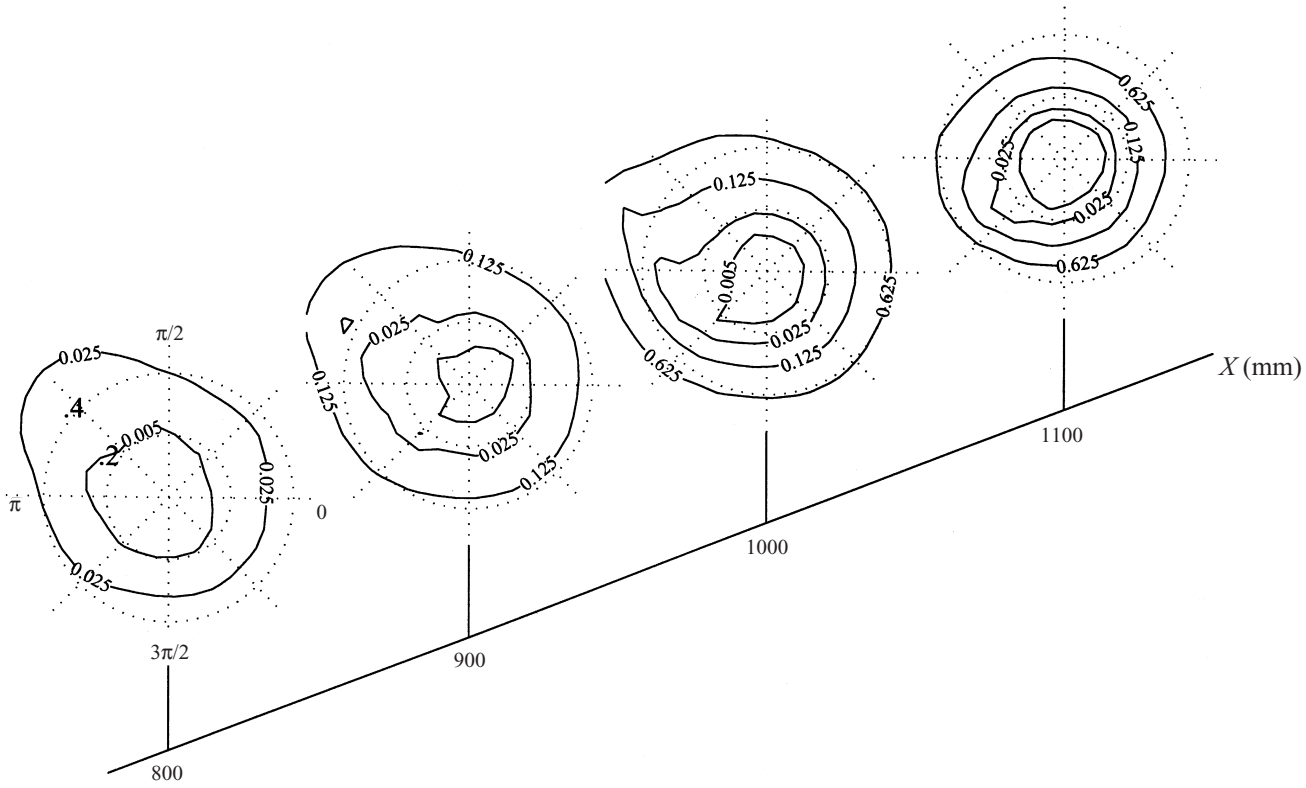


FIGURE 18. Variation of the spectral content of the nonlinearly generated 25th Fourier component of the low-frequency band with respect to the phase and magnitude of the wavepackets for different downstream stations. The dotted lines indicate the phase and magnitude of the complex amplitude of the excitation.

this rotation effect shows is that the phases for which the nonlinear interaction is stronger or weaker depend on the streamwise position where nonlinearity first occurs. This was considered a clear demonstration that the phenomenon observed was not controlled by the local effects of the excitation process. This rotation effect suggests that the important parameter is the phase of the packet with respect to the envelope, which, because of the difference between the group velocity and the phase velocity of the wavepacket components, varies as the disturbance travels downstream. Another aspect of the asymmetry of the contours on figure 18 is that, at each contour level, the phase for which the nonlinear interaction is weakest is very well defined. On the other hand, in the region where the phenomenon is strongest the contour lines exhibit a circular shape indicating that there the nonlinear interaction is of similar magnitude for a wide range of phases.

4. Final remarks

Previous studies have suggested that some aspects of the nonlinear behaviour of modulated three-dimensional Tollmien–Schlichting waves are very different from that of regular plane Tollmien–Schlichting wavetrains. This paper discusses the results of an investigation of the phenomenon in which the wavepacket was used as an example of a modulated wavetrain.

The problem was introduced by the comparison of the evolution of two packets of opposite sign. It was shown that the nonlinear behaviour of these wave systems is remarkably different from one another. It has been suggested that this behaviour could be linked to local effects caused by the excitations close to the source, but these conjectures have not been investigated previously. In the current study, linear correlations of wavepackets of opposite sign indicated that for relatively small excitations the local effects of the excitation process were restricted to a region very close to the source. They did not seem to leave any scar in the packets downstream that could explain the differences found in the nonlinear regime arising from changing the sign of the excitation.

Further studies on the local influence of the excitation process were carried out with excitations of complex amplitudes. First, tests were performed to verify that it was indeed possible to generate the wavepackets from disturbances produced by a loudspeaker in a wind tunnel experiment. It was found that for some wavepackets nonlinear behaviour was observed at remarkably small amplitudes, of roughly 0.2% of the free-stream velocity, whereas for packets of the same magnitude, but opposite sign, the evolution remained essentially linear up to amplitudes twice as large. The experiments showed that the phase of the input that created the earliest sign of nonlinearity was dependent on the excitation amplitude. Moreover, since the phase also evolves downstream, the results suggested that the important parameter is the phase of the ripples relative to the modulation envelope.

The results presented here can also be linked to experiments on more generic types of modulated waves. Shaikh (1993) excited the flow artificially with a disturbance that resembled those generated by the free-stream turbulence. A deterministic white noise signal was fed to the loudspeaker. The excitation had a flat spectrum and a random phase composition. It was observed that the white noise disturbance leads to transition through the generation of turbulent spots in a manner very similar to that observed in natural transition experiments. Shaikh (1993) also found that the early nonlinear stages of the evolution of the noise sequences involve the appearance of waves of frequency lower than the Tollmien–Schlichting band, resembling the

https://doi.org/10.1017/S0022112099006175 Published online by Cambridge University Press

results obtained for wavepackets. The overall view of the results suggested that the wavepackets imitate the natural transition process to a great extent. The experiment was repeated (Shaikh & Gaster 1994) with other white noise sequences of identical spectra but different phase randomization. The results showed that the transition location was remarkably dependent on the phase composition of the white noise sequences. This phenomenon may be linked to the influence of the phase on the evolution of the packets.

The authors want to acknowledge the fruitful discussions with Dr F. N. Shaikh. This work was supported by a grant from CNPq/Brazil, No. 20012691-1 and an ORS Award from the UK.

REFERENCES

Breuer, K. S. & Haritonidis, J. H. 1990 The evolution of a localised disturbance in a laminar boundary layer. Part 1. Weak disturbances. *J. Fluid Mech.* **220**, 569–594.

Cohen, J., Breuer, K. S. & Haritonidis, J. H. 1991 On the evolution of a wave packet in a laminar boundary layer. *J. Fluid Mech.* **225**, 575–606.

Craik, A. D. D. 1971 Nonlinear resonant instability in a boundary layer. *J. Fluid Mech.* **50**, 393–413.

Gaster, M. 1975 A theoretical model of a wave packet in the boundary layer on a flat plate. *Proc. R. Soc. Lond.* A **347**, 271–289.

Gaster, M. 1978*a* The physical process causing breakdown to turbulence. In *12th Naval Hydrodynamics Symposium, Washington.*

Gaster, M. 1978*b* Series representation of the eigenvalues of the Orr–Sommerfeld equation. *J. Comput. Phys.* **29**, 147–162.

Gaster, M. 1984 A non-linear transfer function description of wave growth in a boundary layer. In *Laminar-Turbulent Transition, IUTAM Symposium*, pp. 107–114. Springer.

Gaster, M. & Grant, I. 1975 An experimental investigation of the formation and development of a wavepacket in a laminar boundary layer. *Proc. R. Soc. Lond.* A **347**, 253–269.

Healey, J. J. 1995 A new boundary resonance enhanced by wave modulation: theory and experiment. *J. Fluid Mech.* **304**, 231–262.

Herbert, T. 1988 Secondary instability of boundary layers. *Ann. Rev. Fluid Mech.* **20**, 487–526.

Konzelmann, U. 1990 Numerische Untersuchungen zur räumlichen Entwicklung dreidimensionaler Wellenpakete in einer Plattengrenzschichtströmung. PhD thesis, Universität Stuttgart.

Konzelmann, U. & Fasel, H. 1991 Numerical simulation of a three-dimensional wave packet in a growing flat plate boundary layer. In *Boundary Layer Transition and Control*, pp. 24.1–24.11. The Royal Aeronautical Society, Cambridge, UK.

Medeiros, M. A. F. 1996 The nonlinear behaviour of modulated Tollmien–Schlichting waves. PhD thesis, Cambridge University, UK.

Medeiros, M. A. F. & Gaster, M. 1999 The production of sub-harmonic waves in the nonlinear evolution of wavepackets in boundary layers. *J. Fluid Mech.* (accepted for publication).

Perry, A. E. 1982 *Hot-wire Anemometry*. Clarendon.

Shaikh, F. N. 1993 Turbulent spot in a transitional boundary layer. PhD thesis, Cambridge University.

Shaikh, F. N. & Gaster, M. 1994 The non-linear evolution of modulated waves in a boundary layer. *J. Engng Maths* **28**, 55–71.

https://doi.org/10.1017/S0022112099006175 Published online by Cambridge University Press